Hindawi
Journal of Sensors
Volume 2024, Article ID 9824154, 1 page
https://doi.org/10.1155/2024/9824154

Retraction

Retracted: The Study of Midinfrared Extremely Narrow Dual-Band Absorber Based on a Novel Metamaterial Structure

Journal of Sensors

Received 23 January 2024; Accepted 23 January 2024; Published 24 January 2024

This article has been retracted by Hindawi following an investigation undertaken by the publisher [1]. This investigation has uncovered evidence of one or more of the following indicators of systematic manipulation of the publication process:

(1) Discrepancies in scope
(2) Discrepancies in the description of the research reported
(3) Discrepancies between the availability of data and the research described
(4) Inappropriate citations
(5) Incoherent, meaningless and/or irrelevant content included in the article
(6) Manipulated or compromised peer review

The presence of these indicators undermines our confidence in the integrity of the article's content and we cannot, therefore, vouch for its reliability. Please note that this notice is intended solely to alert readers that the content of this article is unreliable. We have not investigated whether authors were aware of or involved in the systematic manipulation of the publication process.

Wiley and Hindawi regrets that the usual quality checks did not identify these issues before publication and have since put additional measures in place to safeguard research integrity.

We wish to credit our own Research Integrity and Research Publishing teams and anonymous and named external researchers and research integrity experts for contributing to this investigation.

The corresponding author, as the representative of all authors, has been given the opportunity to register their agreement or disagreement to this retraction. We have kept a record of any response received.

References

[1] Z. Li, J. Li, Y. Zhang, Y. Zhai, X. Chu, and Y. Zhang, "The Study of Midinfrared Extremely Narrow Dual-Band Absorber Based on a Novel Metamaterial Structure," *Journal of Sensors*, vol. 2021, Article ID 1048309, 11 pages, 2021.

Hindawi
Journal of Sensors
Volume 2021, Article ID 1048309, 11 pages
https://doi.org/10.1155/2021/1048309

Research Article

The Study of Midinfrared Extremely Narrow Dual-Band Absorber Based on a Novel Metamaterial Structure

Zichun Li, Jinhua Li, Ye Zhang, Yingjiao Zhai, Xueying Chu, and Yu Zhang

International Joint Research Center for Nanophotonics and Biophotonics, Nanophotonics and Biophotonics Key Laboratory of Jilin Province, School of Science, Changchun University of Science and Technology, Changchun, 130022, China

Correspondence should be addressed to Jinhua Li; lijh@cust.edu.cn

Received 1 September 2021; Accepted 6 October 2021; Published 9 November 2021

Academic Editor: Haibin Lv

Due to the problems that the metal pattern layer on the top of the traditional metamaterial structure is easy to be oxidized and easy to fall off, in this paper, a novel semiconductor metamaterial nanostructure composed of a periodic array of GaAs-SiO_2 cubes and a gold (Au) film has been proposed. Using FDTD solutions software to prove this metamaterial structure can achieve ultranarrow dual-band, nearly perfect absorption with a maximum absorbance of 99% and a full-width at half-maximum (FWHM) value that is less than 20 nm in the midinfrared region. The refractive index sensitivity is demonstrated by changing the background index and analyzing the absorption performance. It had been proved that this absorber has high sensitivity (2000/RIU and 1300/RIU). Using semiconductor material instead of the metal material of the top pattern layer can effectively inhibit the performance failure of the metamaterial structure caused by metal oxidation. The proposed narrow, dual-band metamaterial absorber shows promising prospects in applications such as infrared detection and imaging.

1. Introduction

Metamaterials are a class of artificial materials constructed with periodic "meta-atoms" that can be engineered to manipulate electromagnetic waves and produce unconventional optical properties. Since the pioneering work of Pendry [1], several theoretical and experimental demonstrations of functioning electromagnetic metamaterials have been reported [2, 3]. Among these applications, perfect metamaterial absorbers (PMAs) can harvest the power of incident light with nearly 100% efficiency over a wide range of wavelengths [4–6]. These have attracted tremendous research interest after the first investigation by Landy et al. in 2008 [7]. Many PMAs have been proposed, showing practical usage in tasks as diverse as sensing [8], imaging [9], cloaking [10], photodetection [11], photothermal conversion [12], and others [13].

Since Landy et al. proposed the metamaterial structure in 2008, almost all of the metamaterial periodic unit cells have been designed based on the MDM structure. This three-layer structure can achieve perfect absorption by adjusting the geometrical size of the periodic unit structure [14]. However, metamaterial structures composed of metals and dielectrics have two shortcomings. First, a large amount of metal is used that causes the special structure of the top layer to easily oxidize and fall off, and the cost of some precious metals is extremely expensive. Second, owing to the high concentration of free electrons inside the metal, subject to the excitation of external electromagnetic waves, they can produce a variety of surface plasmon resonances [15]. Although high free-electron concentration makes the metal structures of metamaterials easy to achieve perfect absorption, many modes of resonance easily lead to a wider half-width of the absorption peak. At present, to realize the absorption peak of the narrow frequency band [16], it is often necessary to construct a more complicated structure to suppress the resonance absorption of some nonspecific wave bands [17]. This leads to high processing costs and defects in a single preparation method [18]. Compared with traditional metamaterial structures, the novel metamaterials based on semiconductor materials are more sought after by researchers [19]. The novel metamaterial structure based on

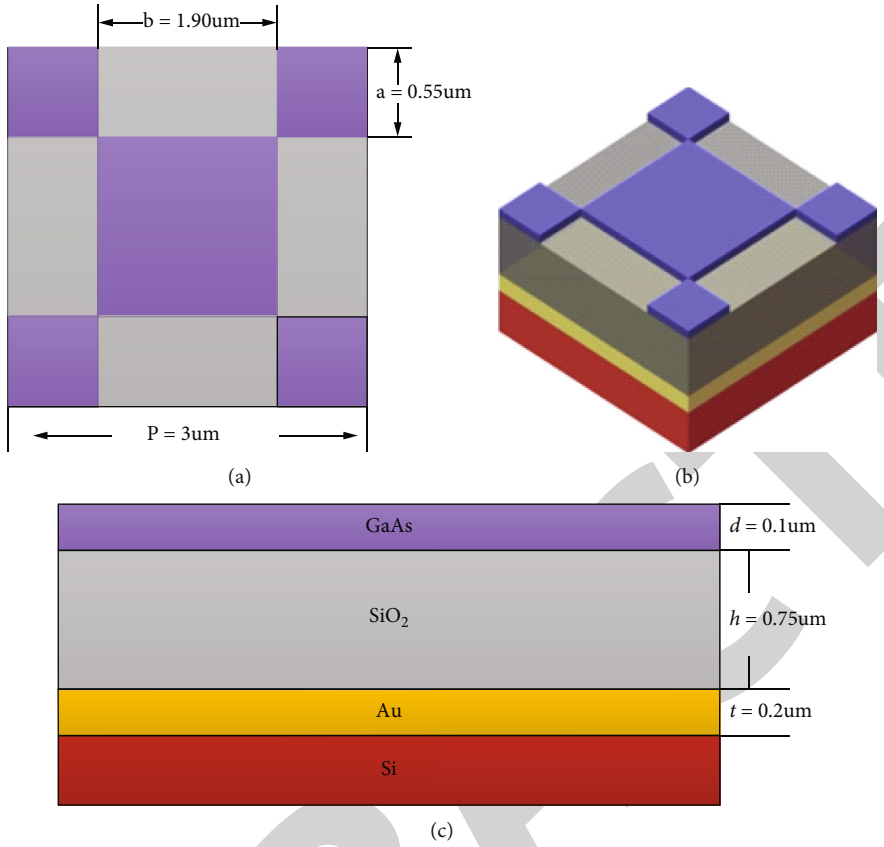

FIGURE 1: (a) Schematic diagram of the top structure of the metamaterial structure. (b) Schematic diagram of the three-dimensional structure of metamaterials. (c) The side view of the metamaterials. $a = 0.55\ \mu m$; $b = 0.95\ \mu m$; $P = 3\ \mu m$; $d = 0.1\ \mu m$; $h = 0.75\ \mu m$; $t = 0.2\ \mu m$.

semiconductor materials can achieve more narrower bands than absorption and more sensitive sensing range than traditional metamaterials [20–22].

In this work, based on the above problems, we propose a new type of semiconductor metamaterial structure that used semiconductor materials instead of the top metal pattern layer. This metamaterial structure can effectively prevent the top pattern layer from being easily oxidized and not closely bonded to the dielectric layer. In this study, gallium arsenide (GaAs) semiconductors (instead of noble metals) are used to synthesize the top layer in a metamaterial structure. GaAs is a novel semiconductor material owing to its metallic and semiconductor properties [23]. Therefore, it could also conduct surface plasmon resonance that will enable the metamaterial structure to achieve perfect absorption characteristics [24]. Because of its lower free electron concentration, the achieved absorption will be extremely narrow [25, 26]. The design is extremely useful for narrowband-responsive bolometers used as focal-plane-array imaging detectors [27]. The detector can also be used for flammable, toxic, and harmful gases such as CH_4, CO, and C_2H_6 in the midinfrared region and SO_2F_2 and SF_6 in the far-infrared [28]. It can also be used in thermal imaging [29], hyperspectral imaging [30], meteorology [31], free-space light [32], communication [33], remote sensing [34], and lasers [35] and for identifying biological compounds [36].

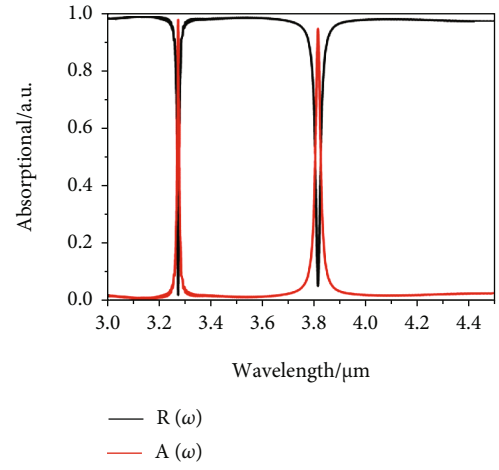

FIGURE 2: Schematic diagram of the resonance absorption peak of the metamaterial structure.

2. Method and Model

2.1. Method. In the numerical simulations, we used finite-difference time-domain (FDTD) methods to solve Maxwell's equations and obtain electric and magnetic field intensities of the surface plasmon resonance of the excitation. The absorption and reflection spectra in the direction

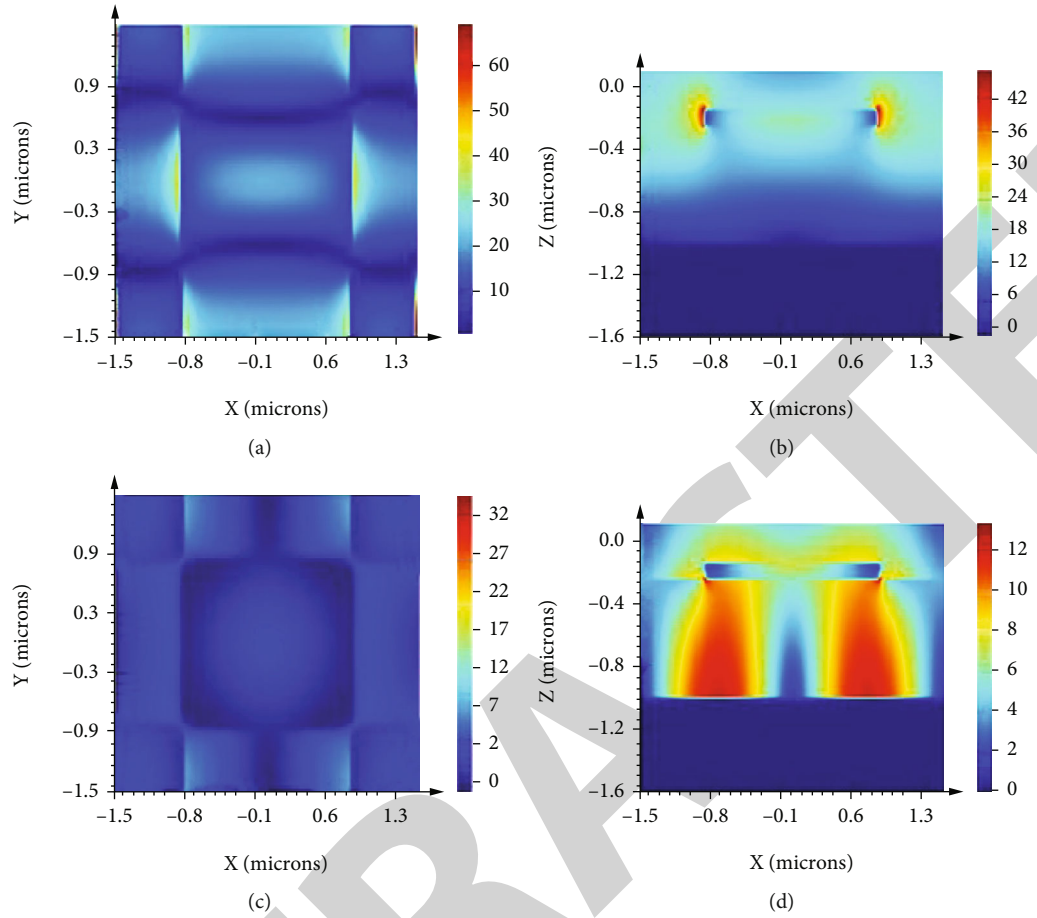

Figure 3: (a, b) The electric field energy distribution diagram of the top structure of the resonance absorption peak at 3.27 μm. (c, d) The electric field energy distribution diagram of the top structure of the resonance absorption peak at 3.81 μm.

perpendicular to an incident electromagnetic wave can be obtained with [37–39]

$$T_\lambda = \frac{\int S(x,y)dxdy}{Q_{\lambda_i}}. \quad (1)$$

In Equation (1), Q is the incident electromagnetic field power per unit area, $S(x,y) = \int_0^T |\vec{E} \times \vec{H}| dt/T$ represents the Poynting vector, and T represents the surface plasmon resonance period. Absorption and transmission peaks can be modeled with Equation (1). Definition A represents the absorbance, where the surface plasmon resonance absorption loss of the incident electromagnetic wave can be defined as

$$A = 1 - T - R. \quad (2)$$

2.2. Model. This metamaterial structure is shown in Figure 1. It has a period $P = 3\,\mu$m, squares at the four corners with side lengths of $a = 0.55\,\mu$m, and a large square structure in the center with a side length of $b = 1.9\,\mu$m. GaAs is shown in blue, the gray area is silica, and its thickness is $d = 0.75\,\mu$m. The metal barrier layer is metal gold. Gold has a very high reflectivity in the infrared band that can ensure that no electromagnetic waves pass through a specific frequency band. During the simulation process, the simulation area is in the midinfrared band (3.0–4.4 μm), the dispersion curve parameter of metal gold is selected from the experimental data measured by Palik, and the dispersion curve of silica is fitted with the dispersion curve that is built in in the commercial software. The dispersion curve of GaAs was also fitted with the experimental data published by Palik. In the simulation process, the light source uses the plane-wave mode. In the XZ direction, the boundary conditions select the perfect matching layer (PML) to allow complete electromagnetic wave emission. Absorption does not have any interference from the simulation results. In the XY plane, the selected boundary condition is a symmetric anti-symmetric periodic boundary condition. The advantage of this boundary condition is to maximize the saving of physical memory, greatly optimize the simulation time, and save memory at the same time. The mesh grid is more refined so that the calculation results are more accurate. The optimization results are shown in Figure 2.

As shown in Figure 2, this novel metamaterial structure produces two resonance absorption peaks with extremely narrow half-widths in the midinfrared range located at 3.27 μm and 3.81 μm, respectively. The half-widths are all less than 10 nm, and the absorption rate is nearly perfect absorption.

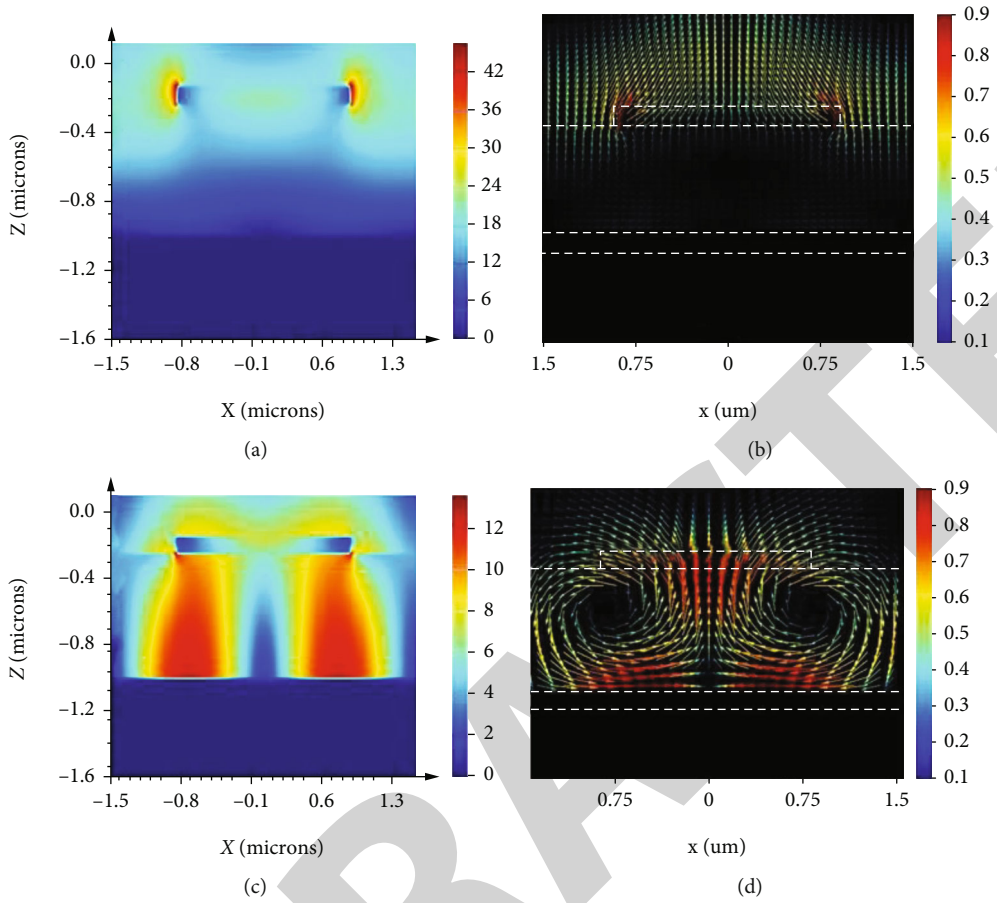

Figure 4: (a, c) The electric field energy distribution diagram of the X-Z plane at 3.27 μm and 3.81 μm. (b, d) The Poynting vector distribution diagram of the X-Z plane absorption peak at 3.27 μm and 3.81 μm.

The absorption mechanism of this metamaterial structure can be analyzed based on the electric field energy level distribution map.

Owing to the limitation of its carrier concentration, a single resonance mode is excited by external electromagnetic waves. From the field energy level distribution diagram, as shown in Figure 3, it can be found that the energy concentration area is extremely symmetrical, indicating that when an electric dipole resonance absorption mode is generated, the electric dipole moment is basically the same; thus, the half-width of the resonance absorption peak is narrower. When a short wavelength electromagnetic wave interacts with a special structure, as shown in Figures 3(a) and 3(b), it can only excite free electrons on the surface of the semiconductor material. Because of the low-carrier concentration, the energy cannot be transferred to the deeper parts of the dielectric layer. Accordingly, the electromagnetic waves of more wavelengths cannot be absorbed. In the longer wavelength frequency domain, as shown in Figures 3(c) and 3(d), the photon energy of the electromagnetic waves cannot effectively excite the resonance mode of the special structure of the top semiconductor. This mode can only be enhanced by exciting the field at the lower surface of the special-shaped structure wherein the dielectric layer contacts the dielectric layer. Therefore, introducing electromagnetic waves of this wavelength into the dielectric layer causes losses. Thus, the mode is also relatively single, resulting in a very narrow half-width of the resonance absorption peak.

In order to study the physical meaning of the two absorption peaks located at 3.27 μm and 3.81 μm in Figure 2, as shown in Figure 4, the magnetic field distribution and Poynting vector distribution in the central section of the metamaterial structure parallel to the X-Z plane at these two wavelengths are shown.

It can be seen from Figure 4 that when the incident light with a wavelength of 3.81 μm irradiates the metamaterial structure, the energy of the incident light is localized in the silica film, and the electric field distribution pattern implies the existence of PSP. As shown in Figure 4, when incident light with a wavelength of 3.27 μm is irradiated on the metamaterial structure, the energy of the incident light is localized in the lattice of the gallium arsenide unit, especially in the slit between the particles. This shows from the side that incident light with a wavelength of 3.27 μm will cause a strong interaction between the gallium arsenide cells. The interaction between the gallium arsenide units relies on the transmission of a strong electric field in the slit.

In order to further clarify the physical meaning of dual-band absorption, we have performed the magnetic field strength and divergence analysis, as shown in Figure 5. When

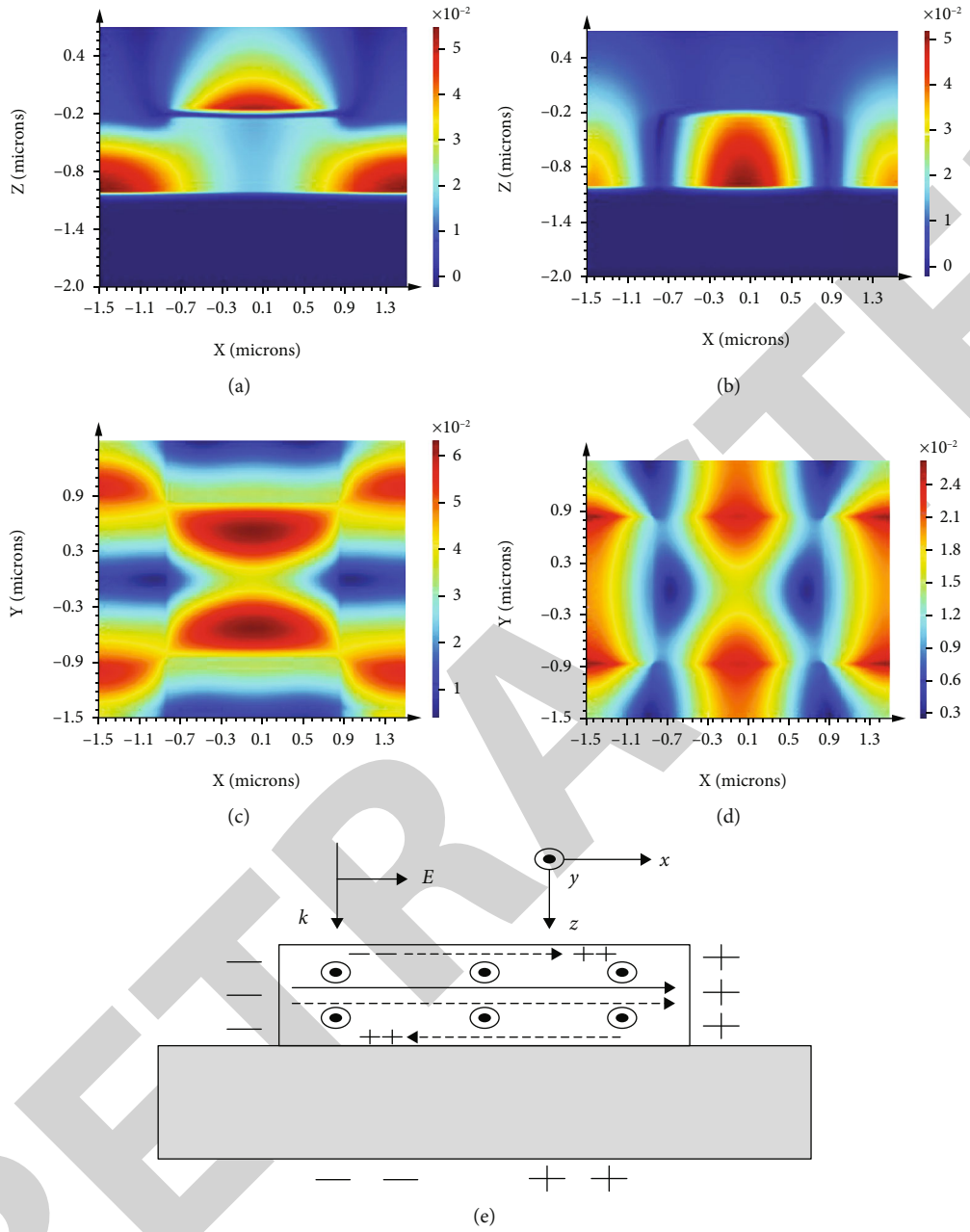

Figure 5: (a, b) The magnetic field energy distribution of the metamaterial structure of the resonance absorption peak at 3.27 μm and 3.81 μm. (c, d) The scatter diagram top view of the top structure of the resonance absorption peak at 3.27 μm and 3.81 μm. (e) Mechanism diagram.

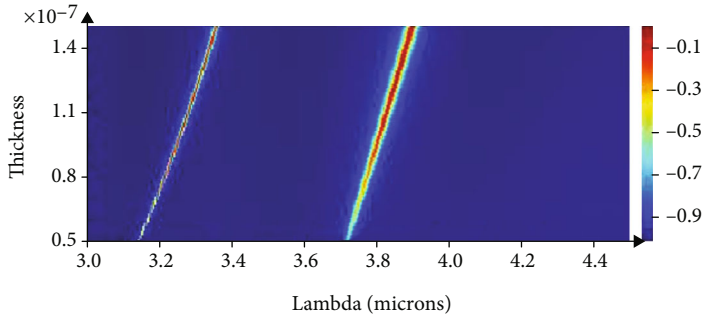

Figure 6: Influence of the thickness of the top structure on the resonance absorption peak.

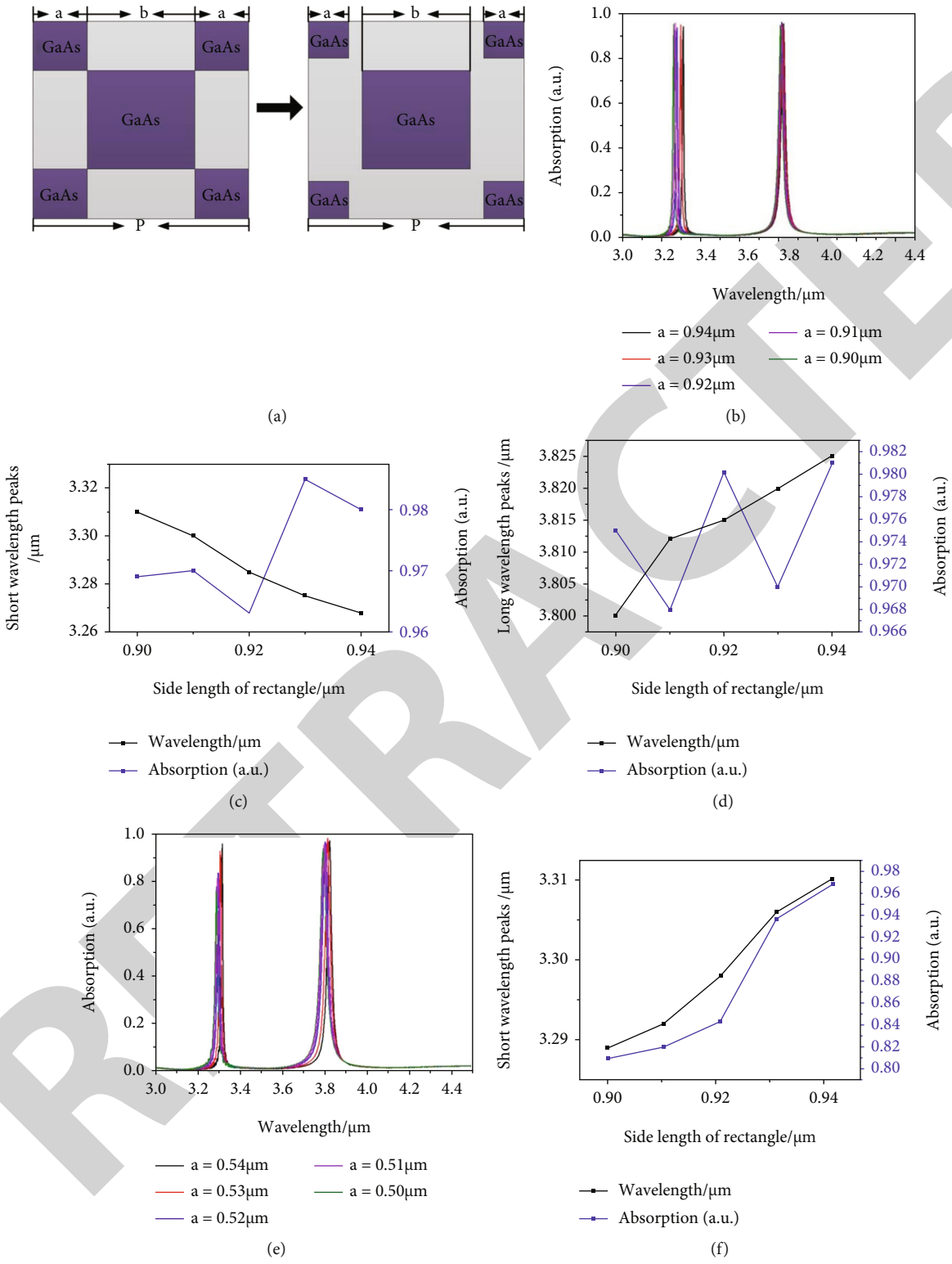

Figure 7: Continued.

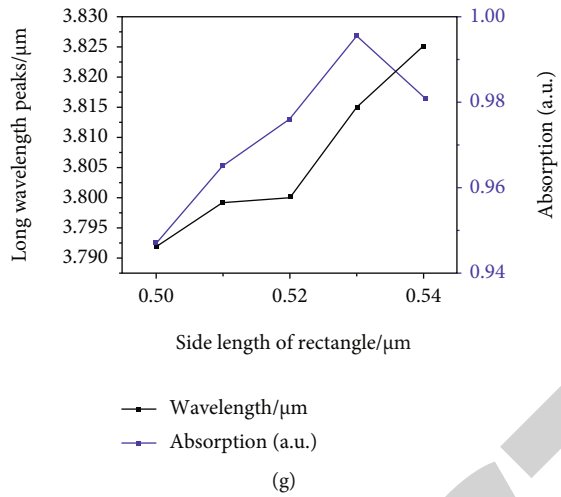

FIGURE 7: The schematic about reduction and increase of the side length of rectangle. (a) Is the schematic diagram of separation. (b) Shows *a* unchanged and *b* reduced; (e) shows *b* unchanged and *a* reduced; (c, d, f, g) central wavelength and absorption rate change trend graph.

incident light with a wavelength of 3.81 μm illuminates the metamaterial structure, because the electromagnetic field form of PSP is a two-dimensional electromagnetic wave bound at the metal-medium interface, the energy of the incident light with a wavelength of 3.81 μm is localized in the form of PSP, inside the silica film. Coincidentally, Figure 4(c) shows that when incident light with a wavelength of 3.27 μm illuminates the metamaterial structure, there is also a collective oscillation of positive and negative polarized charges on the surface of the gold film. However, it can be seen from Figure 4(d) that there are two electron density waves with the same wavelength and opposite propagation directions on the upper surface of the gold film. Therefore, in the silica film, there are two two-dimensional electromagnetic waves with the same wavelength and opposite propagation directions. Destructive interference occurs between them, which explains the disappearance of the electric field inside the silica film, and the electric field is mainly concentrated in the lattice of gallium arsenide cells.

3. Numerical Analysis and Discussion

3.1. Geometric Parameters

3.1.1. Top Layer Thickness. When the thickness of the top layer structure changes, the two resonance absorption peaks exhibit obvious red shifts, as shown in Figure 6. These outcomes indicate that the top and bottom surfaces of the top layer structure have polarized currents in opposite directions. According to Lenz's law, localized surfaces are generated. The collective electron oscillation frequency of the plasmon decreases, and the phenomenon of red shift of the resonance absorption peak then occurs.

3.1.2. Side Length of Rectangle. Considering that the intercept of the two square patterns may not be obvious during the fabrication processing, we have carried out variable control studies on the large rectangle at the center and the small rectangle at the four corners for this situation. Considering that during the fabrication processing, it is easy to produce two situations where the center rectangle and the rectangles at the four corners are separated from each other and overlap each other. Therefore, according to objective facts, we proposed four changes. To fix the center rectangle remaining unchanged, the side length of the rectangle at the four corners is reduced, the side length of the control four-corner rectangle is unchanged, and the side length of the center rectangle is reduced, which leads to the situation that the top corners of the rectangle cannot be perfectly intersected. The change trend schematic is shown in Figure 7(a). In addition, to control the center rectangle remaining unchanged and the side length of the four-corner rectangle increasing, control the four-corner rectangle's side length to remain unchanged, and the side length of the center rectangle increases, which leads to the result that the large and small rectangles overlap each other. The change trend schematic is shown in Figure 8(a).

As shown in Figures 7(b), 7(e), 8(b), and 8(e), by changing the side length of the rectangle, the result is obtained, and it is found that the resonance absorption peak does not change significantly regardless of whether the side length of the rectangle becomes larger or smaller.

As shown in Figures 7 and 8, the center wavelength of the resonant absorption peak does not have a large frequency shift regardless of separation or intersection, and the absorption rate is always higher than 80% within the varying range.

4. Sensitivity Analysis

The resonant absorption peak of a metamaterial is extremely sensitive to changes in the refractive index of the environment. When the background refractive index changes, different metamaterial structures themselves have different responsiveness to changes in the refractive index. This change characteristic is called the sensitivity of the metamaterial. In applications such as optical sensors, metamaterials are required to have extremely high sensitivity. The physical quantity that characterizes the sensitivity of a metamaterial

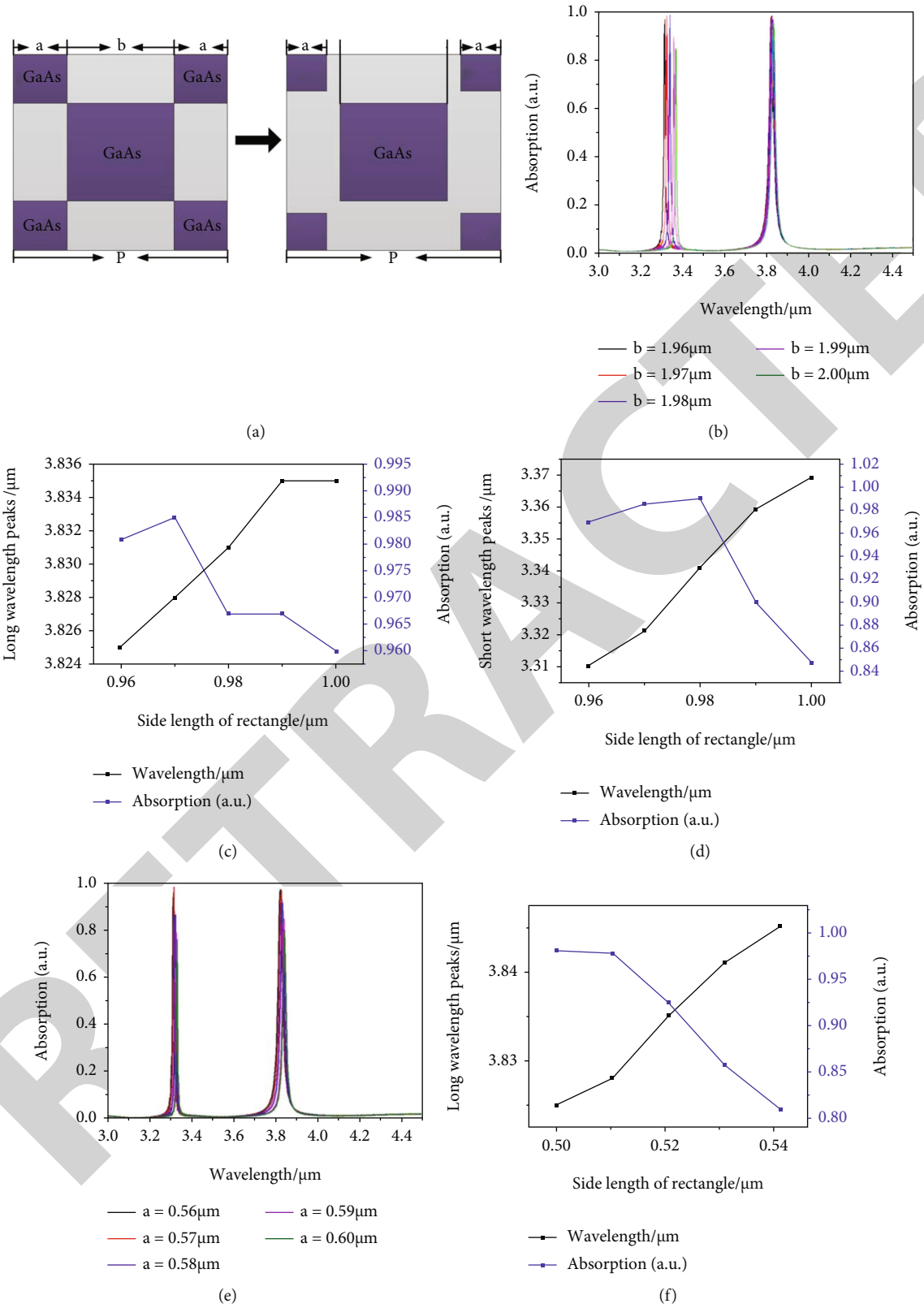

Figure 8: Continued.

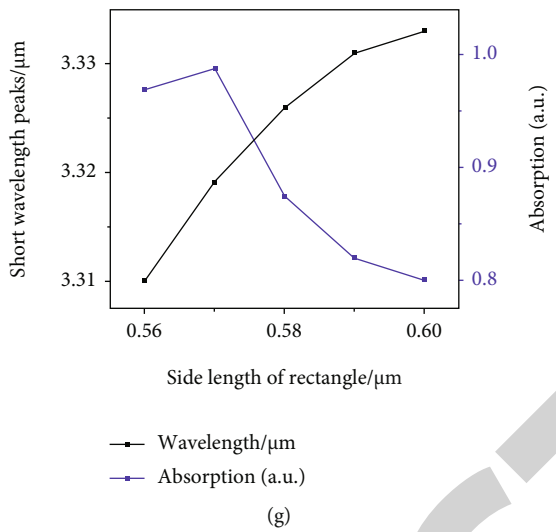

Figure 8: The schematic about reduction and increase of the side length of rectangle. (a) Is the schematic diagram of intersection; (b) shows *a* unchanged and *b* decreased. (e) Shows *b* unchanged and *a* decreased. (c, d, f, g) Shows central wavelength and absorption rate change trend graph.

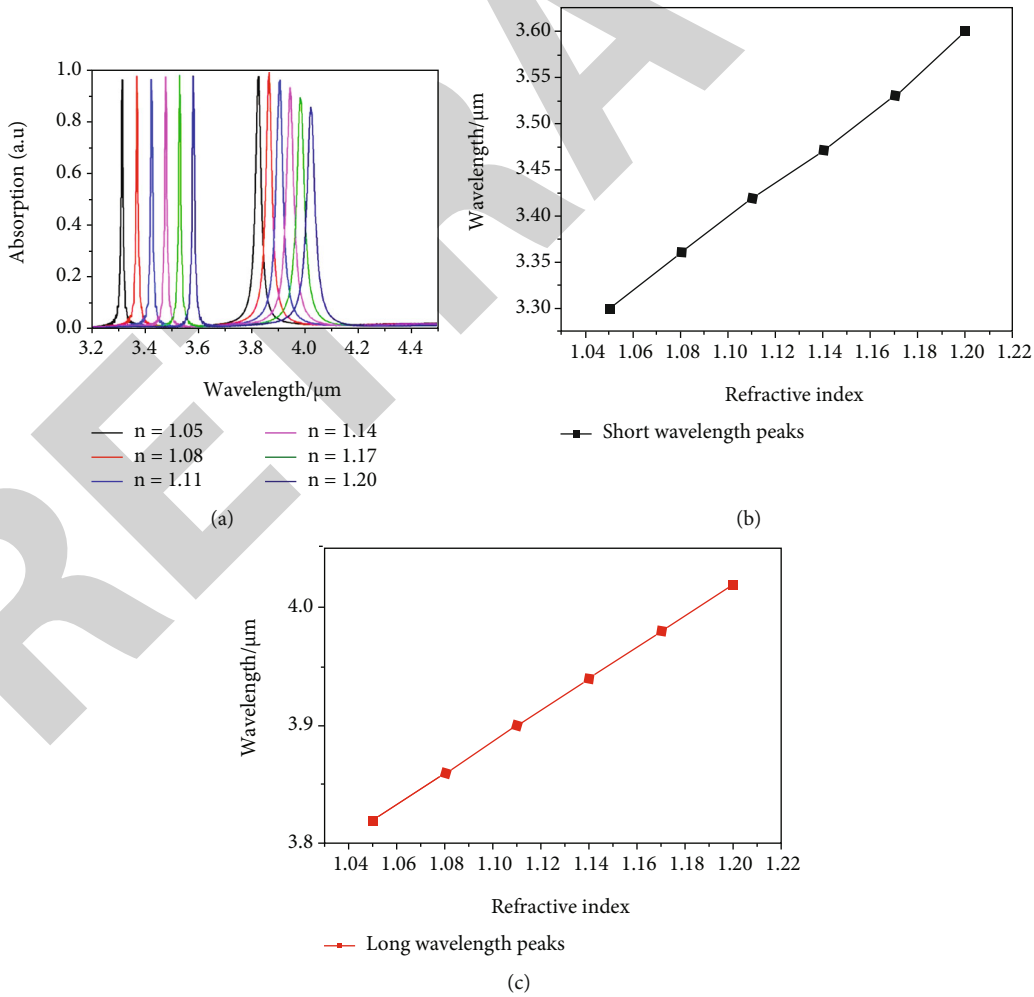

Figure 9: Resonance absorption peak of background refractive index change.

structure is RIS (refractive index sensitivity). $d\lambda$ and dn are the frequency shift and the environmental refractive index unit (RIu) of the absorption peak:

$$\mathrm{RIS} = \frac{d\lambda}{dn}. \quad (3)$$

As shown in Figure 9(a), when the background refractive index changes from 1.05 to 1.2, all the resonance absorption peaks yield obvious red shifts. As shown in Figures 9(b) and 9(c), the resonance absorption peaks at the short wavelength peak position have a frequency shift near 300 nm, while long wavelength peaks are located at a frequency shift near 200 nm. According to Equation (3), the two peaks of absorption RIS are near 2000 nm/RIU and 1300 nm/RIU, respectively.

5. Conclusion

In summary, focus is given to the problems of the metal pattern layer in the traditional metamaterial structure easily oxidized, and the free electron concentration is high; the thermal damping is large. In this paper, a novel metamaterial structure based on semiconductors has been proposed, which is different from the traditional metamaterial structure. The top layer structure of this metamaterial is composed of semiconductor materials. Because semiconductor materials have a low free-electron concentration and are not easy to oxidize, the geometrical dimensions can achieve dual-band resonance absorption characteristics in the midinfrared band by adjusting this periodic structure. Additionally, the two resonance absorption peaks have extremely high sensitivity and excellent quality factors. Because of this special property, this material has tremendous application prospects in both the detection and the imaging fields. Furthermore, because the material used is not a precious metal, it can effectively reduce costs.

Data Availability

The data used to support the findings of this study are included within the article.

Conflicts of Interest

The authors declare that they have no conflicts of interest.

Acknowledgments

This work is supported by the "111" Project of China (D17017), the National Natural Science Foundation of China (21703017), the Developing Project of Science and Technology of Jilin Province (202002040JC, 20200201266JC, 20200201271JC, 20200201060JC, 20200201255JC, and 20190201181JC), the International Science and Technology Cooperation Project of Jilin Province (20190701029GH), and the Project of Education Department of Jilin Province (JJKH20190551KJ and JJKH20200730KJ), the China Postdoctoral Science Foundation (2019M651181), the Youth Fund and Technology Innovation Fund of Changchun University of Science and Technology (XQNJJ-2018-03 and XJJLG-2018-01).

References

[1] J. B. Pendry, "Negative refraction makes a perfect lens," *Physical Review Letters*, vol. 85, no. 18, pp. 3966–3969, 2000.

[2] N. P. Johnson, A. Z. Khokhar, H. M. Chong, R. Rue, T. Antosiewicz, and S. McMeekin, "A review of size and geometrical factors influencing resonant frequencies in metamaterials," *Opto-Electronics Review*, vol. 14, no. 3, pp. 187–191, 2006.

[3] W. Cai, U. K. Chettiar, A. V. Kildishev, and V. M. Shalaev, "Optical cloaking with metamaterials," *Nature Photonics*, vol. 1, no. 4, pp. 224–227, 2007.

[4] T. Chen, S.-J. Li, X.-Y. Cao, J. Gao, and Z.-X. Guo, "Ultra-wideband and polarization-insensitive fractal perfect metamaterial absorber based on a three-dimensional fractal tree microstructure with multi-modes," *Applied Physics A: Materials Science & Processing*, vol. 125, no. 4, 2019.

[5] S.-J. Li, P.-X. Wu, H.-X. Xu et al., "Ultra-wideband and polarization-insensitive perfect absorber using multilayer metamaterials, lumped resistors, and strong coupling effects," *Nanoscale Research Letters*, vol. 13, 2018.

[6] J. Wu, Y. Lu, S. Feng et al., "The interaction between quantum dots and graphene: the applications in graphene-based solar cells and photodetectors," *Advanced Functional Materials*, vol. 28, article 180471, 2018.

[7] N. I. Landy, S. Sajuyigbe, J. J. Mock, D. R. Smith, and W. J. Padilla, "Perfect metamaterial absorber," *Physical Review Letters*, vol. 100, no. 20, 2008.

[8] R. Yahiaoui, S. Tan, L. Cong, R. Singh, F. Yan, and W. Zhang, "Multispectral terahertz sensing with highly flexible ultrathin metamaterial absorber," *Journal of Applied Physics*, vol. 118, no. 8, article 083103, 2015.

[9] K. Lee, H. J. Choi, J. Son, H.-S. Park, J. Ahn, and B. Min, "THZ near-field spectral encoding imaging using a rainbow metasurface," *Scientific Reports*, vol. 5, no. 1, article 14403, 2015.

[10] J. Wang, Y. Jiang, and Z. Hu, "Dual-band and polarization-independent infrared absorber based on two-dimensional black phosphorus metamaterials," *Optics Express*, vol. 25, no. 18, pp. 22149–22157, 2017.

[11] K. K. Paul, N. Sreekanth, R. K. Biroju, T. N. Narayanan, and P. K. Giri, "Solar light driven photoelectrocatalytic hydrogen evolution and dye degradation by metal-free few-layer MoS_2 nanoflower/TiO_2(B) nanobelts heterostructure," *Solar Energy Materials & Solar Cells*, vol. 185, pp. 364–374, 2018.

[12] K. Zhang, M. Z. Peng, W. Wu et al., "A flexible p-CuO/n-MoS_2heterojunction photodetector with enhanced photoresponse by the piezo-phototronic effect," *Materials Horizons*, vol. 4, no. 2, pp. 274–280, 2017.

[13] Y. Jiang, W. Chen, and J. Wang, "Broadband MoS_2-based absorber investigated by a generalized interference theory," *Optics Express*, vol. 26, no. 19, pp. 24403–24412, 2018.

[14] Z. Bai, Y. Liu, R. Kong et al., "Near-field terahertz sensing of HeLa cells andPseudomonasbased on monolithic integrated metamaterials with a spintronic terahertz emitter," *ACS Applied Materials & Interfaces*, vol. 12, no. 32, pp. 35895–35902, 2020.

[15] L. Zhao, H. Liu, Z. He, and S. Dong, "Theoretical design of twelve-band infrared metamaterial perfect absorber by

combining the dipole, quadrupole, and octopole plasmon resonance modes of four different ring-strip resonators," *Optics Express*, vol. 26, no. 10, pp. 12838–12851, 2018.

[16] Q. Zhong, T. Wang, X. Jiang, L. Cheng, R. Yan, and X. Huang, "Near-infrared multi-narrowband absorber based on plasmonic nanopillar metamaterial," *Optics Communication*, vol. 19, 2020.

[17] T. Sang, R. Wang, J. Li, J. Zhou, and Y. Wang, "Approaching total absorption of graphene strips using a c-Si subwavelength periodic membrane," *Optics Communication*, vol. 413, pp. 255–260, 2018.

[18] C. Chen, S.-Y. Yang, J. Yu, R.-X. Xia, L.-X. Zhu, and X.-L. Xu, "Numerical study on tunable perfect absorption in square graphene-dielectric arrays at near-infrared wavelengths," *Materials and Design*, vol. 128, pp. 157–165, 2017.

[19] Y. Wang, X.-F. Xuan, L. Zhu, H.-J. Yu, Q. Gao, and X.-L. Ge, "Numerical study of an ultra-broadband, wide-angle, polarization-insensitive absorber in visible and infrared region," *Optical Materials*, vol. 114, article 110902, 2021.

[20] P. Fu, F. Liu, G. J. Ren, F. Su, D. Li, and J. Q. Yao, "A broadband metamaterial absorber based on multi-layer graphene in the terahertz region," *Optics Communication*, vol. 417, pp. 62–66, 2018.

[21] S.-X. Xia, X. Zhai, Y. Huang, J.-Q. Liu, L.-L. Wang, and S.-C. Wen, "Multi-band perfect plasmonic absorptions using rectangular graphene gratings," *Optics Letters*, vol. 42, no. 15, pp. 3052–3055, 2017.

[22] D. Benedikovic, M. Berciano, C. Alonso-Ramos et al., "Dispersion control of silicon nanophotonic waveguides using sub-wavelength grating metamaterials in near- and mid-IR wavelengths," *Optics Express*, vol. 25, no. 16, pp. 19468–19478, 2017.

[23] D. Huo, J. Zhang, H. Wang et al., "Broadband perfect absorber with monolayer MoS_2 and hexagonal titanium nitride nanodisk array," *Nanoscale Research Letters*, vol. 12, no. 1, 2017.

[24] B. Yosif, M. E. A. Abo-Elsoud, and H. Marouf, "High-performance enhancement of a GaAs photodetector using a plasmonic grating," *Plasmonics*, vol. 15, pp. 1377–1387, 2020.

[25] H. Meng, X. Xue, Q. Lin, G. Liu, X. Zhai, and L. Wang, "Tunable and multi-channel perfect absorber based on graphene at mid-infrared region," *Applied Physics Express*, vol. 11, no. 5, article 052002, 2018.

[26] Y. Li, X. Zhai, S. Xia, H. Li, and L. Wang, "Active control of narrowband total absorption based on terahertz hybrid Dirac semimetal-graphene metamaterials," *Journal of Physics D: Applied Physics*, vol. 53, no. 20, p. 205106, 2020.

[27] Z. Taghipour, V. Rogers, B. Ringel, A. W. K. Liu, and S. Krishna, "Photoluminescence spectroscopy of metamorphic InAsSb on GaAs and Si," *Journal of Luminescence*, vol. 228, article 117581, 2020.

[28] G. Rodrigo Sergio and M.-M. Luis, "Absorption-induced transparency metamaterials in the terahertz regime," *Optics Letters*, vol. 41, no. 2, pp. 293–296, 2016.

[29] Z. Xiaoguang, D. Guangwu, K. Wu, W. Anderson Stephan, and Z. Xin, "Intelligent metamaterials based on nonlinearity for magnetic resonance imaging," *Advanced Materials*, vol. 5, no. 4, pp. 61–68, 2016.

[30] A. Bhardwaj, V. Sridurai, N. M. Puthoor, A. B. Nair, T. Ahuja, and G. G. Nair, "Evidence of tunable fano resonance in a liquid crystal-based colloidal metamaterial," *Advanced Optical Materials*, vol. 1, no. 8, pp. 42–51, 2020.

[31] R. Singh, C. Rockstuhl, and W. Zhang, "Strong influence of packing density in terahertz metamaterials," *Applied Physics Letters*, vol. 97, no. 24, article 241108, 2010.

[32] K. Chen, R. Adato, and H. Altug, "Dual-band perfect absorber for multispectral plasmon enhanced infrared spectroscopy," *ACS Nano*, vol. 6, no. 9, pp. 7998–8006, 2012.

[33] G. Yao, F. Ling, J. Yue, C. Luo, J. Ji, and J. Yao, "Dual-band tunable perfect metamaterial absorber in the THz range," *Optics Express*, vol. 24, no. 2, pp. 1518–1527, 2016.

[34] Y. Su and Z. N. Chen, "A radial transformation-optics mapping for flat ultra-wide-angle dual-polarized stacked GRIN MTM Luneburg lens antenna," *IEEE Transactions on Antennas and Propagation*, vol. 67, no. 5, pp. 2961–2970, 2019.

[35] Y. F. Yang, H. W. Hu, M. J. Wu, T. Y. Lin, J. L. Shen, and Y. F. Chen, "Stretchable and broadband cavity-free lasers based on all 2D metamaterials," *Advanced Optical Materials*, vol. 1, no. 3, pp. 26–33, 2020.

[36] B. Zhongyang and L. Yongshan, "Near-field terahertz sensing of HeLa cells and Pseudomonas based on monolithic integrated metamaterials with spintronic terahertz emitter," *ACS Applied Materials & Interfaces*, vol. 10, no. 20, 2020.

[37] M. Born and E. Wolf, *Principle of Opics*, Cambridge University, 1999.

[38] R. C. Rumpf, "Improved formulation of scattering matrices for semi-analytical methods that is consistent with convention," *Progress In Electromagnetics Research B*, vol. 35, no. 1, pp. 241–261, 2011.

[39] L. Li, "New formulation of the Fourier modal method for crossed surface-relief gratings," *Journal of the Optical Society of America. A*, vol. 14, no. 10, pp. 2758–2767, 1997.